Communication

EPR, UV–Vis, IR, and X-ray Demonstration of the Anionic Dimeric Dinitrosyl Iron Complex [(NO)Fe(□-SBu)Fe(NO)]: Relevance to the Products of Nitrosylation of Cytosolic and Mitochondrial Aconitases, and High-Potential Iron Proteins

Chih-Chin Tsou, Tsai-Te Lu, and Wen-Feng Liaw

J. Am. Chem. Soc., **2007**, 129 (42), 12626-12627• DOI: 10.1021/ja0751375 • Publication Date (Web): 27 September 2007

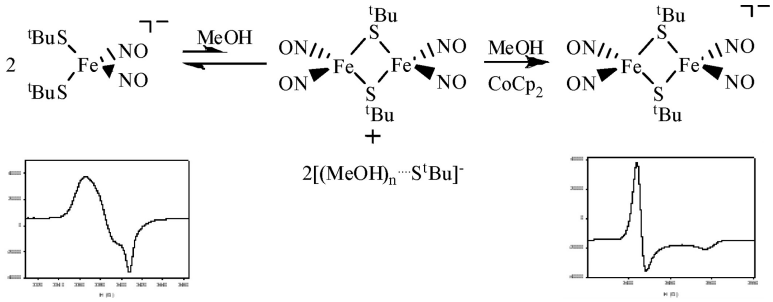

More About This Article

Additional resources and features associated with this article are available within the HTML version:

- Supporting Information
- Links to the 4 articles that cite this article, as of the time of this article download
- Access to high resolution figures
- Links to articles and content related to this article
- Copyright permission to reproduce figures and/or text from this article

View the Full Text HTML

J|A|C|S
COMMUNICATIONS

Published on Web 09/27/2007

EPR, UV−Vis, IR, and X-ray Demonstration of the Anionic Dimeric Dinitrosyl Iron Complex $[(NO)_2Fe(\mu\text{-}S^tBu)_2Fe(NO)_2]^-$: Relevance to the Products of Nitrosylation of Cytosolic and Mitochondrial Aconitases, and High-Potential Iron Proteins

Chih-Chin Tsou, Tsai-Te Lu, and Wen-Feng Liaw*

Department of Chemistry, National Tsing Hua University, Hsinchu 30013, Taiwan

Received July 10, 2007; E-mail: wfliaw@mx.nthu.edu.tw

Dinitrosyl iron complexes (DNICs) are known as one of the two possible naturally occurring forms for storage and delivery of NO in biological systems.[1] NO can be stored in the form of protein-bound DNICs and is probably released from cells in the form of low-molecular-weight DNICs (LMW DNICs).[2] NO release is regulated by ligands coordinated to the $\{Fe(NO)_2\}$ unit.[3a] As has been known, characterization of both protein-bound DNICs and LMW DNICs in vitro is possible via their distinctive electron paramagnetic resonance (EPR) signals at $g = 2.03$.[1,2] Roussin's red esters (RREs), the dimeric form of DNICs considered to perform the similar role as DNICs, are diamagnetic and EPR-silent due to the antiferromagnetic coupling between the two iron centers.[3b,c] Recently, formation of the protein-bound RREs accompanied by protein-bound DNICs (4:1 molar ratio) was observed on the basis of EPR and UV−vis spectra upon nitrosylation of the $[4Fe-4S]^{2+}$ clusters of FNR, a *hmp* gene transcription regulator.[4] In addition, inactivation of cytosolic and mitochondrial aconitases by nitrosylation led to the formation of DNICs displaying the rhombic EPR spectrum with $g = 2.037$, 2.031, 2.012, and an axial EPR spectrum with $g = 2.006$, 1.97 (assigned as a d^9 DNIC) was observed upon the subsequent reduction by excess dithionite.[5]

According to the Enemark and Feltham notation,[6] DNICs can be divided into three major types; monomeric EPR-active $\{Fe(NO)_2\}^9$, EPR-silent $\{Fe(NO)_2\}^{10}$ DNICs, and dimeric EPR-silent/-active $[\{Fe(NO)_2\}^9-\{Fe(NO)_2\}^9]$ DNICs.[3] We have shown that addition of H^+/SR^- to DNICs/RREs, respectively, triggered the interconversion of DNICs and RREs.[3] We also noticed that reduction of RREs yielding the proposed $[Fe_2(\mu\text{-}SR)_2(NO)_4]^-$ (R = Me, Et) with EPR $g = \sim 1.995$ at 250 K and $[Fe_2(\mu\text{-}SR)_2(NO)_4]^{2-}$ characterized by IR and ^1H NMR were reported by Glidewell and Wojcicki, respectively.[7] In this contribution, the anionic dimeric dinitrosyl iron complex $[Fe_2(\mu\text{-}S^tBu)_2(NO)_4]^-$ (**2**) was isolated and characterized by single-crystal X-ray diffraction, EPR, IR, SQUID, and UV−vis, and the dynamic equilibrium between DNIC [cation]-$[(NO)_2Fe(S\text{-}^tBu)_2]$ (cation = PPN (**3-PPN**), Na-18-crown-6-ether (**3-Na**)), and RRE $[Fe_2(\mu\text{-}S^tBu)_2(NO)_4]$ (**1**) in protic solvent (MeOH) due to the hydrogen-bonding formation was also studied.

The THF solution of complex **1**, KC_8, and 18-crown-6-ether was stirred at ambient temperature for 1 h (Scheme 1a); reduction occurred to yield complex [K-18-crown-6-ether][$Fe(\mu\text{-}S\text{-}^tBu)(NO)_2]_2$ (**2**). The IR spectrum of complex **2** exhibits diagnostic υ_{NO} stretching frequencies at 1673 s, 1655 s cm^{-1} (THF) with $\Delta\upsilon_{NO} =$ 18 cm^{-1} ($\Delta\upsilon_{NO}$ = the separation of NO stretching frequencies). The IR spectra for complexes **1** and **2** have the different pattern/position (1802 vw, 1787 s, 1753 s cm^{-1} for **1**) and $\Delta\upsilon_{NO}$ ($\Delta\upsilon_{NO} =$ 27 cm^{-1} for **1**).[8] Compared to complex **1**, which is dominated by three intense absorption bands at 315, 358, 431(sh) nm (THF),[8] complex **2** displays four absorption bands at 310, 435, 639, 982 nm (THF). The UV−vis spectrum of complex **2** exhibits an intense absorption around 982 nm with extinction coefficient >2000 L mol^{-1} cm^{-1} which may be ascribed to the intervalence transition of the fully delocalized mixed-valence complexes (Supporting Information [SI] Figure S1).[9] The temperature-dependent effective magnetic moment (μ_{eff}) decreases from 2.07 μ_B at 300 K to 1.58 μ_B at 4 K (SI Figure S2). At 77 K, complex **2** displays an axial EPR signal at $g_\perp = 2.009$, $g_{||} = 1.965$, and an isotropic EPR signal at $g = 1.998$ at 298 K (Figure 1a,b), deviating from the characteristic EPR signal ($g = 2.03$) of DNICs. Of importance, we noticed that the EPR spectra for complex **2** and the products of reduction of DNIC obtained from nitrosylation of aconitase and reduction of HiPIP-containing protein-bound DNIC had the same pattern and g values.[2a,5]

Scheme 1

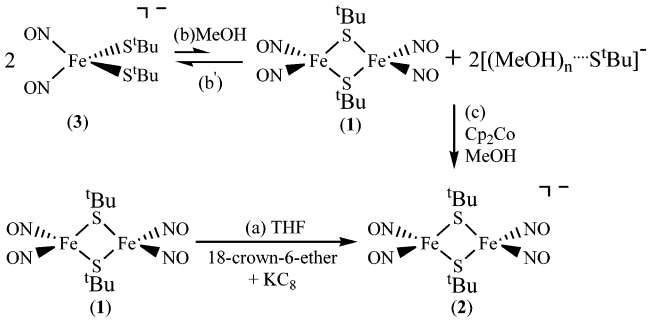

Single-crystal X-ray structure of $[Fe(\mu\text{-}S\text{-}^tBu)(NO)_2]_2^-$ unit in [K^+-18-crown-6-ether] salt is depicted in Figure 2, and selected bond dimensions are presented in the figure caption. The $[Fe(\mu\text{-}S)_2Fe]$ core geometry of complex **2** is best described as a planar rhombus with two *tert*-butyl groups adopting an *anti* configuration in the solid state. The mean N−O bond distances of 1.186(3) Å, (N(1)−O(1) 1.189(3), and N(2)−O(2) 1.183(3) Å) in complex **2**, longer than the average N−O bond distances of 1.1685(19) Å observed in complex **1**, are nearly at the upper end of the 1.178-(3)−1.160(6) Å for the anionic $\{Fe(NO)_2\}^9$ DNICs and nearly at the lower end of the 1.214(6)−1.189(4) Å for the neutral $\{Fe(NO)_2\}^{10}$ DNICs;[10] meanwhile, the mean Fe−N(O) distances of 1.662(2) Å (1.657(2) and 1.666(2) Å) in complex **2** also approach the lower end of 1.695(3)−1.661(4) Å for the anionic $\{Fe(NO)_2\}^9$ DNICs and the upper end of 1.650(7)−1.638(3) Å for the neutral $\{Fe(NO)_2\}^{10}$ DNICs.[10] The apparently longer Fe(1)···Fe(1A) distance (2.9575(8) Å) of complex **2**, compared to the Fe···Fe distance of 2.7049(6) Å in complex **1**,[8] suggests a weaker Fe(1)···Fe(1A) interaction in complex **2**.

Complex [PPN][$(NO)_2Fe(S\text{-}^tBu)_2$] (**3-PPN**) characterized by IR, UV−vis, EPR, and single-crystal X-ray diffraction was isolated

10.1021/ja0751375 CCC: $37.00

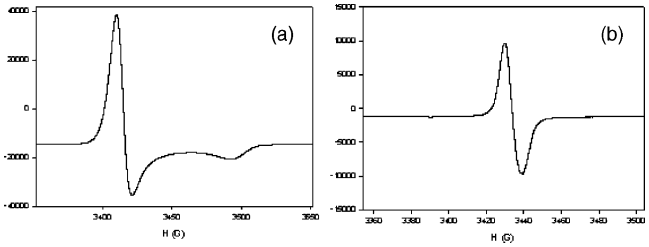

Figure 1. EPR spectrum of complex **2** (a) $g_{\perp} = 2.009$, $g_{\parallel} = 1.965$ at 77 K, and (b) $g_{av} = 1.998$ at 298 K.

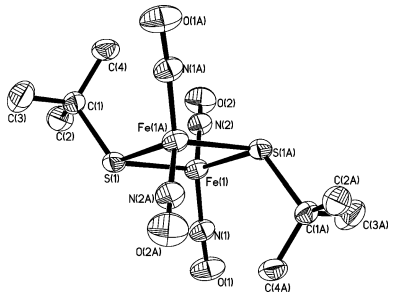

Figure 2. ORTEP drawing and labeling scheme of $[Fe(\mu\text{-}S^tBu)(NO)_2]_2^-$ unit in $[K^+$-18-crown-6-ether] salt with thermal ellipsoids drawn at 50% probability. Selected bond distances (Å) and angles (deg): Fe(1)···Fe(1A) 2.9575(8); Fe(1)−N(1) 1.657(2); Fe(1)−N(2) 1.666(2); Fe(1)−S(1) 2.2991(8); Fe(1)−S(1A) 2.3070(8); O(1)−N(1) 1.189(3); O(2)−N(2) 1.183(3); N(1)−Fe(1)−N(2) 116.08(12); N(1)−Fe(1)−S(1) 107.95(9); N(2)−Fe(1)−S(1) 110.29(9); N(1)−Fe(1)−S(1A) 111.98(9); N(2)−Fe(1)−S(1A) 109.24(9); S(1)−Fe(1)−S(1A) 100.11(3); O(1)−N(1)−Fe(1) 169.9(2); O(2)−N(2)−Fe(1) 169.1(2).

from nitrosylation of the reduced site analogue of rubredoxin protein $[Fe(S^tBu)_4]^{2-}$ in CH_3CN at ambient temperature.[8]

Compared to an isotropic EPR spectrum with signal $g = 2.028$ at 298 K observed in complex $[(EtS)_2Fe(NO)_2]^-$,[11] complex **3-PPN** exhibits a well-resolved five-line EPR signal $g = 2.029$ with hyperfine coupling constants of 2.7 G at 298 K, and high rhombicity with three principal g values of 2.039, 2.027, and 2.013 at 77 K (SI Figure S3a,b). In comparison with complex $[(EtS)_2Fe(NO)_2]^-$ dominated by two intense absorption bands at 436, 802 nm (THF),[11] the electronic spectrum of complex **3-PPN** coordinated by the more electron-donating *tert*-butylthiolate displays a blue-shift to 432, 780 nm. Figure S4 (SI) displays the thermal ellipsoid plot of the anionic complex **3-PPN**, and selected bond distances and angles are given in the figure captions.

Upon dissolution of complex **3-Na** in MeOH at 300 K, the IR spectrum (υ_{NO}: 1806 vw, 1773 s, 1748 s, and 1701 m cm^{-1}) and a rhombic EPR signal with $g = 2.033$ (77 K) (SI Figure S5) implicated the formation of a mixture of complexes **3-Na** and **1** (Scheme 1b). The subsequent addition of 1 equiv of cobaltocene led to the formation of complex **2** characterized by IR and EPR spectra (Scheme 1c) (SI Figure S6). Presumably, the conversion of complex **3-Na** to complex **1** in MeOH was driven by the formation of hydrogen-bonding interactions between the coordinated thiolate ligands of complex **3-Na** and methanol, followed by reduction of complex **1** by cobaltocene to completely yield the stable complex **2** ($E_{1/2} = -1.617$ V (complex **3-Na**), $E_{1/2} = -0.994$ V (complex **1**), $E_{1/2} = -1.353$ V (Cp_2Co) (MeOH)). In contrast to the bridged-thiolate cleavage of RREs $[Fe_2(\mu\text{-}SR)_2(NO)_4]$ by $[SR]^-$ in CH_3CN-producing DNICs $[(RS)_2Fe(NO)_2]^-$ observed in the previous study,[3b] the IR spectrum in the υ_{NO} region shows that the dynamic equilibrium among complexes **3-Na**, **1**, and $[S^tBu]^-$ was reached in 1 h at 300 K when complex **1** and [Na-18-crown-6-ether][S^tBu] in a 1:2 molar ratio were dissolved in CH_3OH. The equilibrium constant, enthalpy, and entropy were calculated to be 3.50×10^{-3} (293 K), 11.5 kJ/mol, and −7.8 J/mol, respectively, by monitoring this equilibrium reaction based upon ^1H NMR spectroscopy (SI Figure S7). The IR spectra in the υ_{NO} region, shifting from 1806 vw, 1773 s, 1748 s, 1701 m cm^{-1} (a mixture of complexes **3-Na** and **1**) to 1743 s, 1698 s cm^{-1} (complex **3-Na**), show the reaction was completely driven to the formation of complex **3-Na** upon further addition of 10 equiv of $[S^tBu]^-$ into the equilibrium MeOH solution of complexes **3-Na**, **1**, and $[S^tBu]^-$ mixture (SI Figure S8).

The EPR spectrum of complex **2**, identical to the EPR spectra of reduction of DNIC/aconitase and HiPIP-containing protein-bound DNIC, demonstrates that nitrosylation of the $[4Fe-4S]^{2+}$ clusters of aconitase/HiPIP produces a mixture of the monomeric and dimeric DNICs.[2a,4−5] The coexistence of a mixture of the monomeric and dimeric DNICs in nitrosylation of aconitase/HiPIP may be ascribed to the initial generation of the monomeric DNICs via nitrosylation of [Fe−S] clusters, followed by the transformation of the monomeric DNICs into the dimeric DNICs driven by the hydrogen-bonding formation between the protic surroundings and DNICs. The EPR-silent dimeric DNICs may be ignored in the nitrosylation of [Fe−S] clusters. Therefore, the EPR spectrum in combination with IR and UV−vis spectra may be employed to serve as an efficient tool to examine the degradation of [Fe−S] clusters via nitrosylation. Study of the interconversion of DNICs, RREs, and anionic RREs is ongoing.

Acknowledgment. We gratefully acknowledge financial support from the National Science Council of Taiwan. We thank Mr. Ting-Shen Kuo and Ms. Chun-Yu Chen for single-crystal X-ray structure determinations.

Supporting Information Available: Experimental details; X-ray crystallographic files in CIF format for the structure determinations of [K-18-crown-6-ether][$Fe_2(\mu\text{-}S^tBu)_2(NO)_4$] and [PPN][$(NO)_2Fe(S\text{-}^tBu)_2$]. This material is available free of charge via the Internet at http://pubs.acs.org.

References

(1) (a) Ueno, T.; Susuki, Y.; Fujii, S.; Vanin, A. F.; Yoshimura, T. *Biochem. Pharmacol.* **2002**, *63*, 485−493. (b) Frederik. A. C.; Wiegant, I. Y.; Malyshev, I. Y.; Kleschyov, A. L.; van Faassen, E.; Vanin, A. F. *FEBS Lett.* **1999**, *455*, 179−182.
(2) (a) Foster, M. W.; Cowan, J. A. *J. Am. Chem. Soc.* **1999**, *121*, 4093. (b) Cooper, C. E. *Biochim. Biophys. Acta* **1999**, *1411*, 290−309.
(3) (a) Tsai, F.-T.; Chiou, S.-J.; Tsai, M.-C.; Tsai, M.-L.; Huang, H.-W.; Chiang, M.-H.; Liaw, W.-F. *Inorg. Chem.* **2005**, *44*, 5872−5881. (b) Tsai, M.-L.; Liaw, W.-F. *Inorg. Chem.* **2006**, *45*, 6583−6585. (c) Tsai, M.-L.; Hsieh, C.-H.; Liaw, W.-F. *Inorg. Chem.* **2007**, *46*, 5110−5117.
(4) Cruz-Ramos, H.; Crack, J.; Wu, G.; Hughes, N. M.; Scott, C.; Thomson, J. A.; Green, J.; Poole, K. R. *EMBO J.* **2002**, *21*, 3235−3244.
(5) Kennedy, M. C.; Anthonline, E. W.; Beinert, H. *J. Biol. Chem.* **1997**, *272*, 20340−20347.
(6) Enemark, J. H.; Feltham, R. D. *Coord. Chem. Rev.* **1974**, *13*, 339−406.
(7) (a) Crayston, A. J.; Glidewell, C.; Lambert, J. R. *Polyhedron* **1990**, *9*, 1741−1746. (b) Chau, C.-N.; Wojcicki, A. *Polyhedron* **1992**, *11*, 851−852. (c) Glidewell, C. *Polyhedron* **1992**, *11*, 2803−2804. (d) Chau, C.-N.; Wojcicki, A. *Polyhedron* **1993**, *12*, 1261−1263.
(8) Harrop, T. C.; Song, D. T.; Lippard, S. J. *J. Am. Chem. Soc.* **2006**, *128*, 3528−3529.
(9) (a) Stebler, A.; Ammeter, J. H.; Fuerholz, U.; Ludi, A. *Inorg. Chem.* **1984**, *23*, 2764−2767. (b) Ondrechan, M. J.; Ko, J.; Zhang, L.-T. *J. Am. Chem. Soc.* **1987**, *109*, 1672−1676.
(10) Hung, M.-C.; Tsai, M.-C.; Lee, G.-H.; Liaw, W.-F. *Inorg. Chem.* **2006**, *45*, 6041−6047.
(11) Lu, T.-T.; Chiou, S.-J.; Chen, C.-Y.; Liaw, W.-F. *Inorg. Chem.* **2006**, *45*, 8799−8806.

JA0751375